Magnetic states of atomic vacancies in graphite probed by scanning tunneling microscopy

Cite as: AIP Advances **10**, 085325 (2020); https://doi.org/10.1063/5.0010466
Submitted: 27 July 2020 . Accepted: 05 August 2020 . Published Online: 24 August 2020

Wonhee Ko, Hyo Won Kim, Yeonchoo Cho, JiYeon Ku, Hyeokshin Kwon, Youngtek Oh, Jin-Wook Jung, Insu Jeon, Hwansoo Suh, Young Kuk, and Sung Woo Hwang

Magnetic states of atomic vacancies in graphite probed by scanning tunneling microscopy

Cite as: AIP Advances 10, 085325 (2020); doi: 10.1063/5.0010466
Submitted: 27 July 2020 • Accepted: 5 August 2020 •
Published Online: 24 August 2020

Wonhee Ko,[1,2,a] Hyo Won Kim,[1] Yeonchoo Cho,[1] JiYeon Ku,[1] Hyeokshin Kwon,[1] Youngtek Oh,[1] Jin-Wook Jung,[1] Insu Jeon,[1] Hwansoo Suh,[1] Young Kuk,[3,4] and Sung Woo Hwang[1]

AFFILIATIONS

[1] Nanoelectronics Lab., Samsung Advanced Institute of Technology, Suwon 16678, South Korea
[2] Center for Nanophase Materials Sciences, Oak Ridge National Laboratory, Oak Ridge, Tennessee 37831, USA
[3] Department of Physics and Astronomy, Seoul National University, Seoul 08826, South Korea
[4] Daegu Gyeongbuk Institute of Science and Technology, Daegu 42988, South Korea

[a] **Author to whom correspondence should be addressed:** kow1@ornl.gov

ABSTRACT

Intrinsic defects in graphitic materials, like vacancies and edges, have been expected to possess magnetic states from the many-body interaction of localized electrons. However, charge screening from graphite bulk carriers significantly reduces the localization effect and hinders the observation of those magnetic states. Here, we use an ultra-low-temperature scanning tunneling microscope with a high magnetic field to observe the magnetic states of atomic vacancies in graphite generated by ion sputtering. Scanning tunneling spectroscopy reveals localized states at the vacancies, which exhibit splitting at a certain magnetic field whose separation increases with the field strength. The transition is well described by the "Anderson model," which describes the emergence of localized magnetic states inside the metallic reservoir through electron–electron interaction. The interaction strength is estimated to be between 1 meV and 3 meV, which is supported by the density functional theory calculation. The observation provides an important foundation for application of intrinsic defects to carbon-based spintronic devices.

I. INTRODUCTION

Carbon-based spintronics have gained large attention because of the long spin-coherence time of electrons from the weak spin–orbit interaction and the absence of a nuclear spin in the most abundant C^{12} nuclei.[1] Although a perfect lattice of sp^2-bonded carbon atoms does not possess any magnetic states, defects such as vacancies and zigzag edges can generate localized states that induce magnetism through the many-body interaction between electrons.[2] The simplest defects in graphene or graphite, namely, vacancies in the size of a few atomic sites, should exhibit spin-split states induced by electron–electron interaction between two electrons with opposite spins.[3] For example, atomic vacancies were generated by irradiating pristine graphene or graphite with ions, and a network of such vacancies exhibited collective magnetic behavior such as ferromagnetism.[4]

Microscopic study of individual vacancies is essential for understanding their magnetism and the role of many-body interaction. Scanning tunneling microscopy/spectroscopy (STM/S) has identified the atomic structure and localized states of vacancies in graphene and graphite;[5–9] however, vacancy states that are split into two spin-polarized states, which is the hallmark of a magnetic state, have not been observed. Recent studies into other defects such as edges[10] and adatoms[11] have revealed that the interaction between defects and the underlying substrate significantly affects the electronic state, and hence, minimizing hybridization between them (e.g., by using an insulating substrate) is important for retaining the magnetic properties of the defects. Graphite can be considered as graphene on top of a graphite substrate weakly bound by van der Waals interaction, and this weak interaction preserves the electronic properties of vacancies better than other metal substrates, as evidenced by sharp vacancy states with an energy broadening of only a

few millielectronvolts.[5,6] Observation of the spin splitting of vacancy states, however, requires an extreme energy resolution (i.e., finer than the broadening which is typically in a millielectronvolt range), thus making operating temperatures lower than 1 K a necessity.

In this study, we use ultra-low-temperature STM to observe the spin-split states of atomic vacancies in highly oriented pyrolytic graphite (HOPG). To see the fine structure of spin splitting, we employed an operating temperature of the millikelvin range to maximize the energy resolution and applied a high magnetic field to increase any existing spin splitting through the Zeeman effect.[12–14] The vacancy state exhibited splitting when a magnetic field was larger than a certain magnitude. The evolution of this splitting with the magnetic field is well described by the "Anderson model,"[15] which describes the transition of localized states from non-magnetic to magnetic that is induced by electron–electron interaction. The interaction strength was estimated to be between 1 meV and 3 meV. Density functional theory (DFT) calculations of multi-layer graphene have shown that spin splitting reduces with the number of layers, which explains the small interaction strength observed in the experiment.

II. EXPERIMENTAL METHODS

For STM/S measurements, we utilized a custom-built dilution-fridge-based ultra-low-temperature scanning tunneling microscope with a base temperature of 10 mK and a magnetic field B of up to 15.4 T.[16,17] During the measurement, the sample temperature was kept below 30 mK to achieve sub-millielectronvolt energy resolution (see Fig. S1 and supplementary material, Sec. 1 for the energy resolution measured on the superconducting gap). The HOPG sample was cleaved in the air and then transferred to the UHV chamber (~10^{-10} Torr) where it was annealed at 200 °C for 30 min for degassing. To create vacancy defects, HOPG was irradiated for 10 s with Ar^+ ions by a sputtering ion gun at an ion energy of 140 eV and under an Ar pressure of 2×10^{-6} Torr.[5,6] Once irradiated, the sample was annealed at 600 °C for 1 h to remove any intercalated impurities.[18] A conventional lock-in technique was used to measure the differential conductance dI/dV with a modulation voltage amplitude (i.e., half of the peak-to-peak voltage) of 200 μV–500 μV and a modulation frequency of 793 Hz. For DFT calculation, we used the Vienna *Ab Initio* Simulation Package with the Perdew–Burke–Ernzerhof exchange correlation functional and D3 dispersion correction.[19–21] The cutoff energy used for the plane-wave basis set was 400 eV. The number of k-points sampled was increased until there was negligible change in the density of states (DOS), and the atomic structure was fully relaxed until the residual force was less than 0.02 eV/Å. A Gaussian broadening of 0.04 eV was applied when calculating the DOS.

III. RESULTS

A. Spin-split states of atomic vacancies measured by STM/STS

Figure 1(a) shows a typical topograph of the HOPG after Ar^+ ion irradiation. Among the various types of defects that are visible, our focus here is on those with a triangular shape as this is the shape

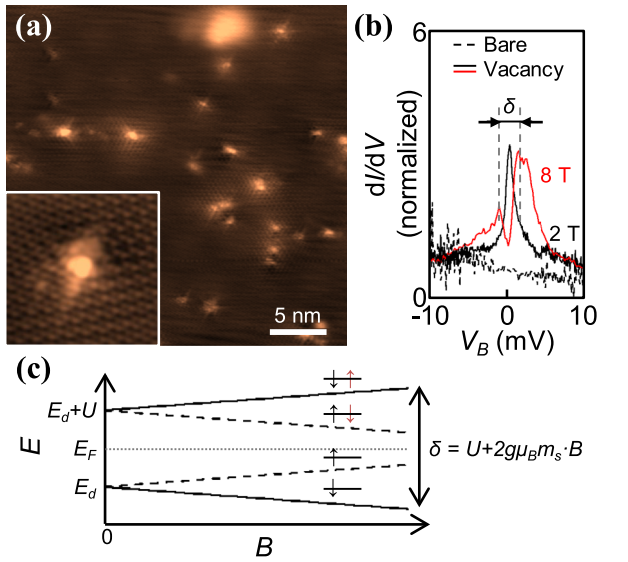

FIG. 1. (a) Topograph of the HOPG surface after Ar^+ ion irradiation (V_B = 300 mV and I = 0.3 nA). The inset at the left bottom corner shows an atomic vacancy at atomic resolution (image size 4 × 4 nm^2, V_B = 100 mV, and I = 0.5 nA). (b) dI/dV spectra taken from the bare surface at B = 0 T (dotted line) and a single vacancy at B = 2 T and B = 8 T (black and red solid line, respectively). The modulation voltage was 200 μV for the bare surface and the vacancy spectrum at 2 T and 500 μV for the vacancy spectrum at 8 T. (c) The energy diagram of the vacancy state with respect to the external magnetic field. The bottom two levels below E_F are the energies for the first electron filling the vacancy state with an opposite spin (black arrow), while the top two levels above E_F correspond to the energies for the second electron filling the same vacancy state (red arrow).

expected of an atomic vacancy [inset of Fig. 1(a)]. Moreover, the atomic vacancies can have various configurations from the distinct arrangement of the carbon lattice and possible hydrogenation due to the high reactivity of the vacancy sites, which can turn the localized vacancy states on or off.[8,22] To identify the vacancies with the localized states, we employed STS to observe the characteristic dI/dV spectra, which are proportional to the local density of states (LDOS), with a peak at about the Fermi energy from the π-band vacancy state (see Fig. S2 and supplementary material, Sec. 2).[3,5–9] The peak of the vacancy state exhibits some variation in amplitude and width due to the polycrystalline nature of HOPG that induces local variation of doping and carrier concentration. Among the several vacancies we observed, the vacancies with a smaller peak width display more prominent splitting with the magnetic field. Figure 1(b) shows an example of the dI/dV spectra taken from the top of a vacancy with the narrowest FWHM of 1.2 meV (black solid line). No splitting of the peak was observed for the magnetic field smaller than 3 T. The thermal broadening and bias modulation is much less than the peak width, which suggests that the observed broadening is intrinsic. At a high magnetic field of B = 8 T, however, the peak of the vacancy state splits into two, with each peak above and below the Fermi level [Fig. 1(b), red solid line]. In contrast, the vacancy states with the FWHM of 8 meV does not show any splitting up to 15 T (see Fig. S3 and supplementary material, Sec. 3).

To explain the vacancy state split, we considered a simple case of the Anderson model where the vacancy state is a single quantum state that two electrons with an opposite spin can occupy. Following the Anderson model, the Hamiltonian H can be separated into four parts:[2,11,15]

$$H = H_{bulk} + H_{vacancy} + H_{Zeeman} + H_{hybrid},$$

where H_{bulk} is the energy of the bulk graphite states, $H_{vacancy}$ is the energy of the vacancy states including electron–electron interaction, H_{Zeeman} is the Zeeman splitting, and H_{hybrid} is the hybridization between bulk graphite states and vacancy states. Here, we focus on the energy diagram of $H_{vacancy}$ and H_{Zeeman} [Fig. 1(c)] because bulk states are not of interest in this paper, so H_{bulk} and H_{hybrid} can be omitted by fixing the Fermi level and giving some broadening Δ to the vacancy states.[15] Then, the many-body interaction is reduced to the two-body interaction with the contracted Hamiltonian H as

$$H = H_{vacancy} + H_{Zeeman} = E_d \sum_{\sigma} n_{d\sigma} + U n_{d\uparrow} n_{d\downarrow} + g\mu_B m_S B(n_{d\downarrow} - n_{d\uparrow}),$$

where E_d is the energy of vacancy states, U is the strength of electron–electron interaction by Coulomb repulsion, $n_{d\sigma}$ is the number operator of vacancy states as defined by $n_{d\sigma} \equiv {c_{d\sigma}}^{\dagger} c_{d\sigma}$, ${c_{d\sigma}}^{\dagger}(c_{d\sigma})$ is the creation (annihilation) operator, g is the g-factor, μ_B is the Bohr magneton, and m_S is the spin quantum number. In all, there are four eigenenergies for the contracted Hamiltonian, i.e., $E_d - (+)\ g\mu_B m_S B$ and $E_d + U - (+)\ g\mu_B m_S B$ for spin down (up) states.[23] Owing to the Pauli exclusion principle, two electrons should have opposite spins, so spin splitting can have two possible values: $\delta = U + 2g\mu_B m_S B$ and $\delta^* = U - 2g\mu_B m_S B$. Only δ is observed in our case because the Fermi level is located between E_d and $E_d + U$ and it forces the first electron to occupy the ground state of the spin pointing down. When electron–electron interaction is present, then $U > 0$, so δ becomes larger than the conventional Zeeman splitting of $2g\mu_B m_S B$. It is known that $g = 2$ in graphite and $m_S = 1/2$ for a single vacancy,[3,24–26] and therefore, the estimated Zeeman splitting is ~0.9 meV at $B = 8$ T. Because this is much smaller than the measured δ of 2.6 meV, as shown in Fig. 1(b), $U > 0$ and electrons in the vacancy state are indeed affected by electron–electron interaction.

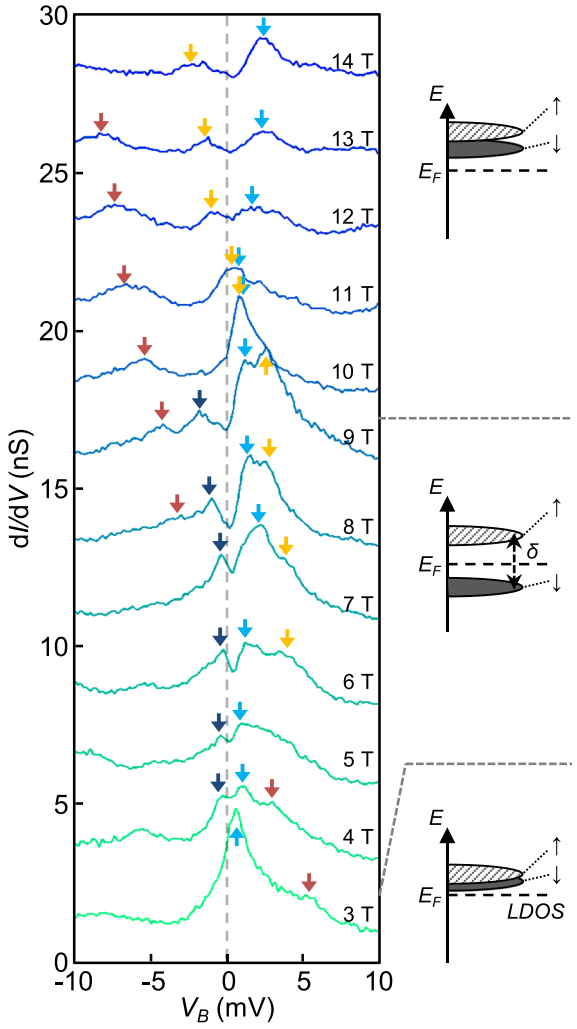

FIG. 2. dI/dV spectra taken from the center of the vacancy while changing the magnetic field from 3 T to 14 T. The modulation voltage was 500 μV for all spectra. Each spectrum is vertically displaced for clarity. The right side depicts the energy diagram of the spin-split states of vacancy at different magnetic field regimes.

B. Magnetic field dependence of the spin-split states

The behavior of the vacancy state in a magnetic field was further investigated by tracking the dI/dV spectra while changing the magnetic field incrementally (Fig. 2). When the magnetic field is increased, several peaks in addition to the one from the vacancy state appear in the dI/dV spectra. These peaks can be broadly categorized into two sets: ones that are always present at around the Fermi energy and shifts less than 0.5 mV/T (dark and light blue arrows in Fig. 2) and others that move monotonically to a negative bias with a step larger than 1 mV/T (red and yellow arrows in Fig. 2). The behavior of the first set is consistent with the vacancy state, while that of the second set is consistent with the bulk states of graphite, such as the Landau levels that are expected to move monotonically with the magnetic field.[27,28] As a control experiment, we measured the dI/dV spectra on the pristine HOPG surface while ramping the magnetic field. The peaks appear when the magnetic field is applied and shift monotonically to a negative bias with a step of about 1 mV/T –2 mV/T, suggesting that they indeed originate from the bulk graphite states (see Fig. S4 and supplementary material, Sec. 4).

The peaks from the vacancy state exhibit a complicated behavior with an increasing magnetic field. For instance, only a single peak appears near the Fermi level up to a field strength of 3 T, but when the field strength exceeds 4 T, the peak splits into two peaks, above and below the Fermi level. This separation also increases with field strength. In real space, the separation of the peaks was constant over the vacancy region and only the amplitude of the peaks changed (see Fig. S5 and supplementary material, Sec. 5), so the splitting δ can be defined as the separation between the peaks. At $B = 4$ T, $\delta = 1.2$ meV, which is comparable to the intrinsic broadening; thus, any splitting below 3 T appears to be disguised by the intrinsic

broadening. The increase in splitting with field strength indicates that the two peaks are spin-polarized states with opposite spins. However, at 10 T and above, the peak below the Fermi level suddenly disappears and only the one above the Fermi level survives. This sudden disappearance of the peak is another indication that the splitting is not just the Zeeman effect of a single electron state but rather the combined electron–electron interaction of a two-body state. For electron–electron interaction to be present, the position of the Fermi level should be between the split vacancy states.[15] In Fig. 2, the center of the vacancy state is monotonically shifted to a positive bias with increasing magnetic field. When the vacancy state energy drifts too far away from the Fermi level, electron–electron interaction should disappear and the splitting significantly decreases in the amount of U, which seems to happen between 9 T and 10 T. It is uncertain why the vacancy state energy shifts with magnetic field, but a shift in the Dirac point of graphite or few-layer graphene with the magnetic field has been observed previously and explained by the charge transfer between the adjacent layers.[28–30] It is expected that the vacancy state energy should follow this shift.

For further quantitative analysis, the energy of the spin-split states and their separation were extracted and plotted in Figs. 3(a) and 3(b), respectively. The peak separation δ from 4 T to 9 T is about three-times as large as the Zeeman splitting in the case of all the extracted values, which provides strong evidence for the presence of electron–electron interaction. The magnitude of U was in the range of 1 meV–3 meV and increased with the magnetic field. It is uncertain at this point why U increases, but one possibility is that it is caused by a reduction in the hybridization between the vacancy state and bulk graphite states due to a quantization of bulk states to Landau levels at higher magnetic fields.[15,30] The appearance and the disappearance of vacancy state splitting at B = 4 T and 10 T are well explained by the Anderson model.[15] According to this model, there are at least two conditions that must be met for the emergence of a localized magnetic state, namely, $U > \pi\Delta$ and $|E_d - E_F| < U$, where 2Δ is the FWHM of the localized state. In our case, $\Delta \approx 0.6$ meV, so spin-split states can appear when $U > 1.8$ meV. Because U increases with the magnetic field, it should eventually cross the threshold when B = 4 T and U = 0.7 meV, at which point the vacancy state becomes magnetic. Differences in the value of U may originate from the detailed structure of the graphite states. At 10 T, $E_d - E_F \approx 1$ meV and becomes comparable to U, so the electron–electron interaction is removed and splitting disappears. Note that all transitions occur at an energy scale of 1 meV, which supports our claim that U is in the range of 1 meV–3 meV.

We note that other possibilities for the abnormally large splitting, such as the higher vacancy magnetic moment or Kondo effect, were carefully checked and excluded. For example, had the spin of the vacancy state been 3/2 rather than 1/2, then the splitting should have increased continuously for all magnetic fields from 3 T to 14 T, and more than two peaks should have appeared at higher magnetic fields. A change in the g-factor for the vacancy state from 2 would also be in contradiction with the reported magnetic property measurements.[7,25] Other many-body interactions, such as the Kondo effect, can cause a larger splitting than the Zeeman effect,[31] but these usually appear as a peak pinned to the Fermi level that does not shift, which is in contrast to our observation and other reports on the graphene vacancy state.[6,32] We also note that the localized spin states can induce inelastic spin–flip excitation that appears as a splitting of a peak at the Fermi level.[33] However, the inelastic feature should have a step-like shape instead of peaks, and the size of splitting should follow the Zeeman splitting of 1/2 spin, which does not correspond to our data. The absence of inelastic spin–flip is probably due to the metallic graphite substrate, which significantly broadens the feature and disguises it.

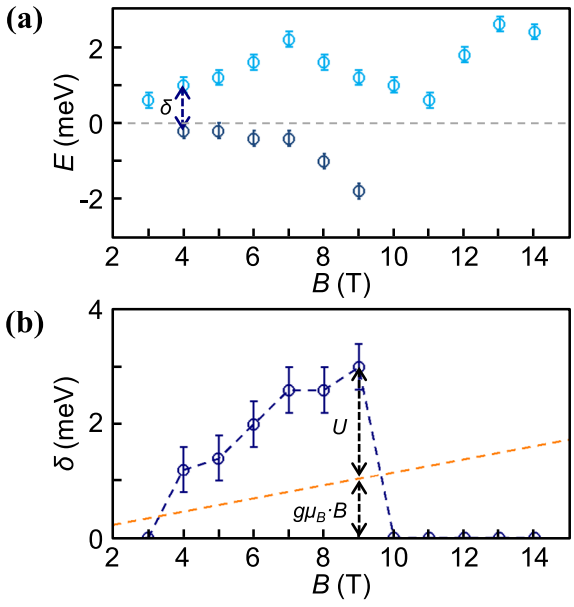

FIG. 3. (a) Energy of spin-split states at the Fermi level, as extracted from the d*I*/d*V* spectra shown in Fig. 2. (b) The separation between spin-split states calculated from (a). Zeeman splitting of m_S = 1/2 is marked as an orange dotted line for comparison. The error bar in (a) and (b) is from minimum spacing between bias voltage points, 200 μV, while obtaining the d*I*/d*V* spectra.

C. DFT calculations of vacancy states in graphite

To verify the origin of U, we also estimated its value through DFT calculations and compared this to the experimental data. However, as HOPG is composed of more than a few tens of Bernal-stacked graphene layers, its simulation is impractical. Instead, we used a vacancy on Bernal-stacked multilayer graphene and tried to find the relation between the number of graphene layers N_L (from one to five) and spin splitting δ (note that $\delta \approx U$ because there is no magnetic field). Splitting is expected to decrease with increased hybridization between the vacancy state and bulk graphite states,[15,34] so a larger N_L should result in a smaller δ. Figure 4(a) shows the atomic structure of a single vacancy on trilayer graphene (N_L = 3) and the LDOS of its majority spin states near the Fermi level (see supplementary material, Sec. 6). A significant portion of the LDOS is located at the first layer beneath the vacancy (18% of the top layer) and even the second layer beneath it (10% of the top layer), indicating that there is a notable amount of hybridization of the vacancy state with the states in the layers beneath it. Spin splitting calculated from the spin-polarized DOS shows a clear decreasing tendency with N_L [see Fig. 4(b) and Fig. S6], and although it is uncertain as to

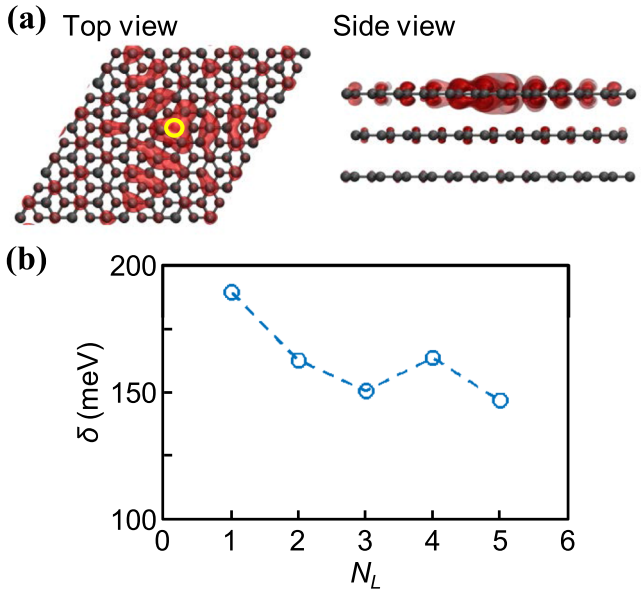

FIG. 4. (a) Atomic structure and the LDOS of a single vacancy on trilayer graphene. The yellow circle denotes the vacancy site. The red surface is an iso-surface of the LDOS, which is calculated for the majority spin state of the vacancy. (b) Spin splitting of the vacancy state with respect to the number of graphene layers.

how far this would continue, if the tendency is retained up to large $N_L \gg 10$, it would be possible for spin splitting to reach a value of a few millielectronvolts.

IV. CONCLUSIONS

In summary, spin splitting of an atomic vacancy of graphite under a high magnetic field has been observed with STM. Electron–electron interaction was identified through the fact that the separation of the splitting was larger than the Zeeman effect and that the splitting only appeared when the vacancy state is near the Fermi level. The electron–electron interaction strength U was measured to be between 1 meV and 3 meV, which is greatly reduced from the expected value of graphene vacancy due to the hybridization between vacancy states and bulk graphite states. The observation that simple intrinsic defects like atomic vacancies can behave as magnetic states would provide important information for the realization of carbon-based spintronic devices or spin-qubit quantum computers.[1]

SUPPLEMENTARY MATERIAL

See the supplementary material for additional STM data and DFT results.

AUTHORS' CONTRIBUTIONS

W.K. and H.W.K. contributed equally to this work.

ACKNOWLEDGMENTS

The data analysis and manuscript writing were conducted at the Center for Nanophase Materials Sciences, which is a DOE Office of the Science User Facility. The authors would like to acknowledge Seongjun Park for the assistance provided via helpful discussions.

DATA AVAILABILITY

The data that support the findings of this study are available from the corresponding author upon reasonable request.

REFERENCES

[1] W. Han, R. K. Kawakami, M. Gmitra, and J. Fabian, Nat. Nanotechnol. **9**, 794 (2014).
[2] O. V. Yazyev, Rep. Prog. Phys. **73**, 056501 (2010).
[3] O. V. Yazyev and L. Helm, Phys. Rev. B **75**, 125408 (2007).
[4] P. Esquinazi, D. Spemann, R. Höhne, A. Setzer, K. H. Han, and T. Butz, Phys. Rev. Lett. **91**, 227201 (2003).
[5] M. M. Ugeda, I. Brihuega, F. Guinea, and J. M. Gómez-Rodríguez, Phys. Rev. Lett. **104**, 096804 (2010).
[6] M. M. Ugeda, D. Fernández-Torre, I. Brihuega, P. Pou, A. J. Martínez-Galera, R. Pérez, and J. M. Gómez-Rodríguez, Phys. Rev. Lett. **107**, 116803 (2011).
[7] S. Just, S. Zimmermann, V. Kataev, B. Büchner, M. Pratzer, and M. Morgenstern, Phys. Rev. B **90**, 125449 (2014).
[8] M. Ziatdinov, S. Fujii, K. Kusakabe, M. Kiguchi, T. Mori, and T. Enoki, Phys. Rev. B **89**, 155405 (2014).
[9] Y. Zhang, S. Y. Li, H. Huang, W. T. Li, J. B. Qiao, W. X. Wang, L. J. Yin, K. K. Bai, W. Duan, and L. He, Phys. Rev. Lett. **117**, 166801 (2016).
[10] P. Ruffieux, S. Wang, B. Yang, C. Sánchez-Sánchez, J. Liu, T. Dienel, L. Talirz, P. Shinde, C. A. Pignedoli, D. Passerone, T. Dumslaff, X. Feng, K. Müllen, and R. Fasel, Nature **531**, 489 (2016).
[11] H. González-Herrero, J. M. Gómez-Rodríguez, P. Mallet, M. Moaied, J. J. Palacios, C. Salgado, M. M. Ugeda, J.-Y. Veuillen, F. Yndurain, and I. Brihuega, Science **352**, 437 (2016).
[12] A. A. Khajetoorians, B. Chilian, J. Wiebe, S. Schuwalow, F. Lechermann, and R. Wiesendanger, Nature **467**, 1084 (2010).
[13] A. F. Otte, M. Ternes, K. Von Bergmann, S. Loth, H. Brune, C. P. Lutz, C. F. Hirjibehedin, and A. J. Heinrich, Nat. Phys. **4**, 847 (2008).
[14] K. von Bergmann, M. Ternes, S. Loth, C. P. Lutz, and A. J. Heinrich, Phys. Rev. Lett. **114**, 076601 (2015).
[15] P. W. Anderson, Phys. Rev. **124**, 41 (1961).
[16] Y. J. Song, A. F. Otte, V. Shvarts, Z. Zhao, Y. Kuk, S. R. Blankenship, A. Band, F. M. Hess, and J. A. Stroscio, Rev. Sci. Instrum. **81**, 121101 (2010).
[17] Model JDR-500, Janis Research Company, Inc., Wilmington, MA.
[18] H. W. Kim, W. Ko, J. Ku, I. Jeon, D. Kim, H. Kwon, Y. Oh, S. Ryu, Y. Kuk, S. W. Hwang, and H. Suh, Nat. Commun. **6**, 7528 (2015).
[19] G. Kresse and J. Furthmüller, Phys. Rev. B **54**, 11169 (1996).
[20] J. P. Perdew, K. Burke, and M. Ernzerhof, Phys. Rev. Lett. **77**, 3865 (1996).
[21] S. Grimme, J. Antony, S. Ehrlich, and H. Krieg, J. Chem. Phys. **132**, 154104 (2010).
[22] M. Casartelli, S. Casolo, G. F. Tantardini, and R. Martinazzo, Carbon **77**, 165 (2014).
[23] F. Manicini and F. P. Mancini, Eur. Phys. J. B **68**, 341 (2009).
[24] G. Wagoner, Phys. Rev. **118**, 647 (1960).
[25] R. R. Nair, M. Sepioni, I.-L. Tsai, O. Lehtinen, J. Keinonen, A. V. Krasheninnikov, T. Thomson, A. K. Geim, and I. V. Grigorieva, Nat. Phys. **8**, 199 (2012).
[26] K. Matsubara, T. Tsuzuku, and K. Sugihara, Phys. Rev. B **44**, 11845 (1991).
[27] G. Li and E. Y. Andrei, Nat. Phys. **3**, 623 (2007).

[28]T. Matsui, H. Kambara, Y. Niimi, K. Tagami, M. Tsukada, and H. Fukuyama, Phys. Rev. Lett. **94**, 226403 (2005).
[29]D. L. Miller, K. D. Kubista, G. M. Rutter, M. Ruan, W. A. De Heer, P. N. First, and J. A. Stroscio, Science **324**, 924 (2009).
[30]H. Min, S. Adam, Y. J. Song, J. A. Stroscio, M. D. Stiles, and A. H. MacDonald, Phys. Rev. B **83**, 155430 (2011).
[31]Y. H. Zhang, S. Kahle, T. Herden, C. Stroh, M. Mayor, U. Schlickum, M. Ternes, P. Wahl, and K. Kern, Nat. Commun. **4**, 2110 (2013).
[32]J. Mao, Y. Jiang, D. Moldovan, G. Li, K. Watanabe, T. Taniguchi, M. R. Masir, F. M. Peeters, and E. Y. Andrei, Nat. Phys. **12**, 545 (2016).
[33]A. J. Heinrich, J. A. Gupta, C. P. Lutz, and D. M. Eigler, Science **306**, 466 (2004).
[34]J. J. Palacios and F. Ynduráin, Phys. Rev. B **85**, 245443 (2012).